Chinese Journal of Chemical Engineering 55 (2023) 156–164

Contents lists available at ScienceDirect

Chinese Journal of Chemical Engineering

journal homepage: www.elsevier.com/locate/CJChE

Full Length Article

Efficient, continuous oxidation of durene to pyromellitic dianhydride mediated by a V-Ti-P ternary catalyst: The remarkable doping effect

Da Ke, Minjia Wang, Jiancheng Ruan, Xinzhi Chen, Shaodong Zhou *

College of Chemical and Biological Engineering, Zhejiang Provincial Key Laboratory of Advanced Chemical Engineering Manufacture Technology, Zhejiang University, Hangzhou 310027, China
Institute of Zhejiang University – Quzhou, Quzhou 324000, China

ARTICLE INFO

Article history:
Received 18 February 2022
Received in revised form 14 March 2022
Accepted 20 March 2022
Available online 26 April 2022

Keywords:
Continuous oxidation
Anhydride
C—H activation
V-Ti-P ternary catalyst

ABSTRACT

Continuous preparation of pyromellitic dianhydride (PMDA) from durene has been studied using a fixed-bed reactor. The reaction was performed using a phosphorus-vanadium-titanium ternary catalyst. Relatively high selectivity and yield of PMDA was obtained. The *in-situ* characterization was combined with theoretical calculation to reveal the reaction mechanisms, and the remarkable doping effect was discussed.

1. Introduction

Pyromellitic anhydride (PMDA) continues to play important roles in chemical industry as it serves as the raw material or key intermediate in the production of diverse plastics, binders, propellants and films [1,2]. Direct oxidation of durene to PMDA is regarded as an ideal route. In recent decades, vanadium has been widely employed as the main active component in the oxidation of various alkanes and arenes like methanol [3], ethanol [4], *n*-butane [5], *o*-xylene [6] *etc*. In particular, the vanadium-titanium binary catalyst can catalyze the oxidation of durene and *o*-xylene to produce PMDA and phthalic anhydride (PA) [7], respectively. Among all oxidation methods [8–11], the method for preparing PMDA from trimethylbenzene is disadvantageous due to the high cost; while the pinacol route is of low cost, its is limited by the low productivity; the yield of PMDA *via* liquid-phase oxidation of durene is relatively high, yet the use of acidic solvent is corrosive and high-pressure oxygen atmosphere is unsafe in scaled-up processes. By contrast, continuous oxidation process carried out in a fixed-bed reactor does not require the presence of organic solvent and is thus eco-friendly. However, the over-oxidation of the raw material is a tricky problem, and selective generation of anhydride is still challenging.

The V atom interacts with Ti *via* two modes, V—Ti and V—O—Ti, and the vanadium oxide species is dispersed on the surface of TiO_2 *et al.* [12]. According to Akbari *et al.* [13], the acid-base active sites on the surface of the V/Ti catalyst play an important role in the oxidation of methyl aromatics, the selectivity increases with the decreasing of acidic sites, but the conversion reduces. The activity of V/Ti catalyst can be improved by adding a third component as promoter, Hutching *et al.* [14] proposed that promoters can modulate the crystal structure and facilitate the formation of sosoloid. For example, Ballarini *et al.* [15] believed that cesium can accelerate the reoxidation process of the reduced vanadium sites during the reaction, which is beneficial to the desorption and adsorption of intermediate compounds. Moreover, phosphorus, argentum, kalium and other elements could also improve the catalytic performance of the V/Ti catalyst [16–19]. In addition, the activity of the V/Ti catalysts also relies on the preparation method. Research shows that catalysts prepared by sol–gel method and atomic-layer deposition have better performance than those prepared by impregnation [20–22]. During the reaction process, excessive reduction of active vanadium sites, carbon deposition, surface sintering and transformation of crystal phase would cause catalyst deactivation [23].

In this work, the V-Ti-P ternary catalyst is prepared by the impregnation method, and highly selective production of anhydride is thus facilitated. Characterization with XRD, XPS, Raman,

* Corresponding author at: College of Chemical and Biological Engineering, Zhejiang Provincial Key Laboratory of Advanced Chemical Engineering Manufacture Technology, Zhejiang University, Hangzhou 310027, China.
E-mail address: szhou@zju.edu.cn (S. Zhou).

https://doi.org/10.1016/j.cjche.2022.03.026
1004-9541/

BET *etc.* has been performed to explore the function of P in the catalyst. The associated origins of the doping effect are discussed.

2. Experimental

2.1. Catalyst preparation

The impregnation method was used to prepare the V-Ti-P catalyst. For a typical procedure, a certain amount of NH_4VO_3 (Aladdin, China, AR) and $H_2C_2O_4$ (Sinopharm, China, AR) are dissolved in deionized water at 85 °C. Then desired amount of phosphoric acid (Sinopharm, China, 85%) is added into the system under stir; after 2 h, TiO_2 (Sinopharm, China, AR) is added and stirring for another 4 h. Finally, the excess water was evaporated by rotary evaporation. The obtained powder is molded to columnar, dried in oven at 120 °C for 4 h and calcined at 500 °C in air for 9 h. A series of V-Ti-P catalysts were prepared by changing the amount of phosphoric acid added. These catalysts are thus named VTP-*x* (*x* means the molar ratio of P to V). For more details, see the Supplementary Material.

2.2. Catalyst characterization

The X-ray diffraction (XRD) patterns were measured at room temperature using D/max-rA with Cu-K_α radiation generated at 10 mA and 40 kV. Raman spectra were measured by Renishaw inVia using 532 nm laser excitation. The X-ray photoelectron spectroscopy (XPS) analysis was carried out by using Thermo Scientific K-Alpha with Al-K_α radiation. BET surface area and pore size distribution were measured on a Micromeritics PHS-1020 (PHSCHINA) system at −196 °C using N_2 as the adsorbate. Before measurements, the samples were degassed at 300 °C for 6 h. The FTIR spectra were recorded on a Nicolet 5700-FTIR (Fourier transform infrared) equipped with a MCT/A detector cooled by liquid N_2 and the light transmission range was 5000–500 cm^{-1}. Additional characteristic data are provided in the Supplementary Material.

2.3. Catalyst activity measurement

The reaction shown in Fig. 1 was carried out in a fixed-bed reactor with salt-bath under atmosphere. About 150 g catalyst was loaded in the reactor and the durene vapor was fed into the device by air. The gas hour space velocity (GHSV) was controlled by air flow rate and the heat power for the vaporization of durene vapor (For technical details, see Supplementary Material). The reaction selectivity was addressed quantitatively using high performance liquid chromatography (Agilent 1000). Note that the by-products of small molecules, such as H_2O, CO, and CO_2 were not counted in, and the selectivity obtained in this work reflects only to the branching ratio of the aromatic products. Turnover frequency (TOF) is calculated by the amount of target product per second per gram of catalyst and the total V atoms in the reactor.

For *in situ* FTIR study on the reaction, about 0.15 g catalyst powder was placed in reaction cell, the reaction mode was consistent with fixed-bed reaction. The GHSVs of durene and air were 4.5 h^{-1} and 1400 h^{-1}, respectively.

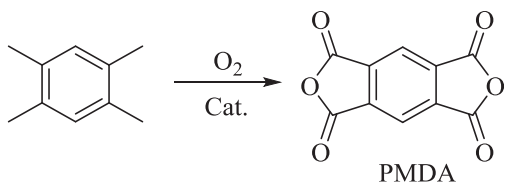

Fig. 1. The oxidation of durene to PMDA.

3. Results and Discussion

3.1. Characterization of the catalyst

3.1.1. X-ray diffraction pattern

The XRD patterns of all the catalysts are shown in Fig. 2. The diffraction of V_2O_5 (standard card#41-1426) is present in all samples, and the ratio of rutile and anatase remains constant except for VTP-1.2 (the detailed amount is provided in Supplementary Material). Noted that, when the P element is introduced into the catalysts, the diffraction of $VOPO_4$ (2θ = 11.9°, 28.7°, 29.1°, 36.1°, 41.3°) becomes clearer; the proportion of $VOPO_4$ is highest in VTP-1. This means the existence of P changes the V species that V_2O_5 partially translates to $VOPO_4$ while not stoichiometrically.

3.1.2. Raman

Raman spectra analysis were performed to obtain further structural information of each sample, and the result is shown in Fig. 3. The strong bands at 702 cm^{-1} and 998 $cm^{-1}$are ascribed to V_2O_5 [24], and the V_2O_5 phase decreases gradually with the addition of P. The result is consistent with XRD pattens. The characteristic peaks located at 892 cm^{-1}, 990 cm^{-1}, 1017 cm^{-1}, 1075 cm^{-1} are

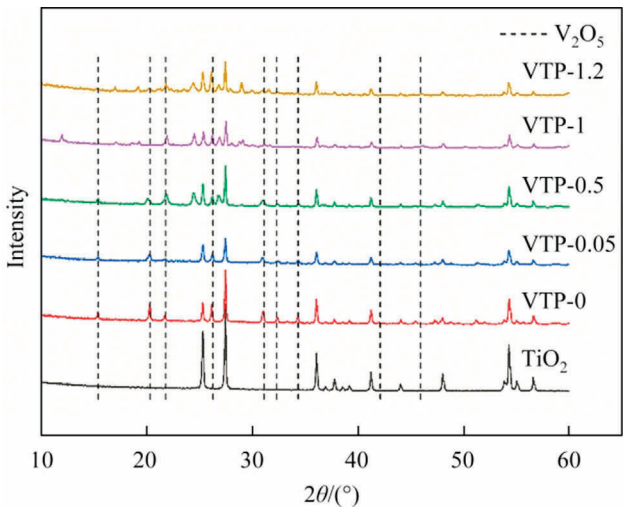

Fig. 2. XRD patterns of VTP-*x* catalyst: the molar ratio of V and Ti in all samples are 1:2.

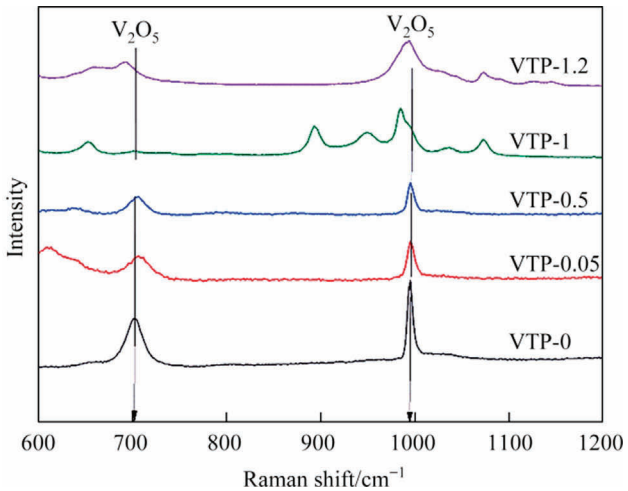

Fig. 3. Raman spectra of VTP-*x* catalyst: 600–1200 cm^{-1}.

attributed to $VOPO_4$ [25], obvious vibration peaks of $VOPO_4$ were not found in VTP-0.05 and VTP-0.5. By contrast, VTP-1 and VTP-1.2 spectra revealed the existence of $VOPO_4$. Interestingly, the bands of $(VO)_2P_2O_7$ (940 cm^{-1}) were detected in VTP-1 catalyst, which was not found in the XRD spectra. Thus, VTP-1 and VTP-1.2 are structurally obviously different from the other samples.

3.1.3. XPS

The surface elemental composition and the oxidation state of all the catalysts were tested by XPS. Fig. 4 shows the oxidation state of O and V. The binding energy of V $2p_{3/2}$ is around 517 eV, and there are two obvious peaks after fitting (Fig. 5), 517.0–517.7 eV and 516.0–516.5 eV; the latter can be attributed to V^{5+} and V^{4+}, in line with the previous reports [26,27]. The detailed data is listed in Table 1, indicating that with the addition of P the content of V^{5+} is slowly increasing. However, too much P results in a much higher content of V^{4+}. Further, the binding energy of the O 1s increases after adding P, which implies a tighter binding of O with the other elements.

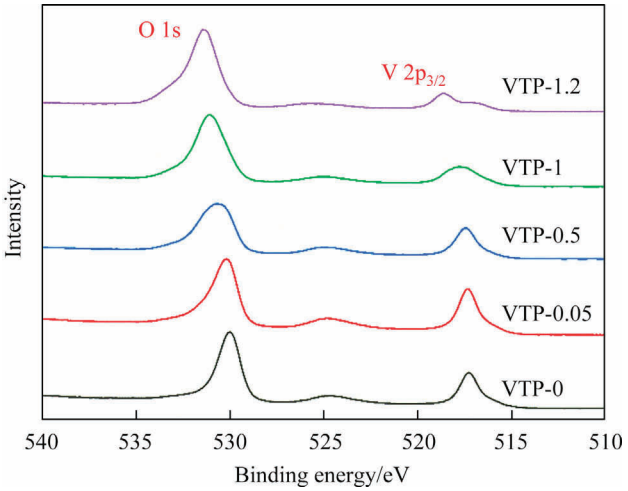

Fig. 4. XPS spectra at the region of O 1s and V 2p.

3.1.4. Bet surface and area and pore size

Table 2 lists the textural parameters of each catalyst and VTP-1 after the catalytic reaction. It is clear that the introducing certain amount of P increases the specific surface area, average pore size and pore volume while decreases them dramatically when further adding P. This may be caused by the formation of $VOPO_4$, and the TiO_2 support might be changed when too much P is introduced. In general, smaller pore size is beneficial for absorption and desorption of the reactants and products. The average pore size and pore volume of VTP-1 sample declined evidently after being used for about 300 h compared with the fresh one. This means coke deposits happened during the reaction process and the activity of catalyst would be influenced.

3.2. Catalyst activity

Catalytic oxidation of durene was carried out continuously in a fixed bed reactor, and the results are shown in Table 3. It is obvious that when appropriate amount of P is added (VTP-1), the product yield is improved notably upon simultaneous enhancement of conversion and selectivity. When the molar ratio of P to V was 1.2, the yield was decreased from 76.80% to 64.69% and for TOF, the value of VTP-1 is higher than and other samples. Most likely, this is related to the surface composition and the ratio of V^{5+}/V^{4+} in each sample: a higher valence of V exerts the catalyst higher oxidizablility.

The temperature and GHSV are crucial to the reaction, and the oxidation reaction with VTP-1 at 340–460 °C and different GHSV was tested in this work (Fig. 6). The optimal reaction temperature was found to be 400 °C. The lower the temperature is, the higher the branching ratio of C—C activation products is. Obviously, as compared to the generation of anhydride *via* multiple C—H activa-

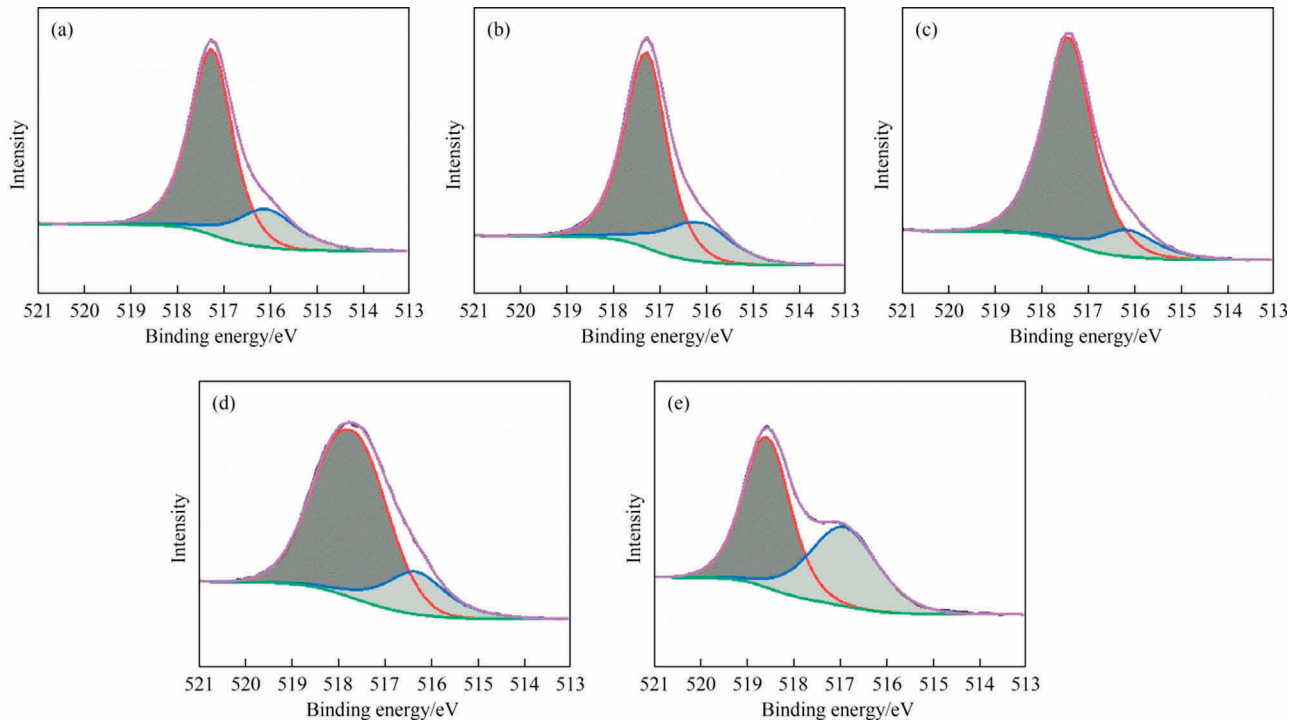

Fig. 5. XPS spectra at the region of V $2p_{3/2}$, (a)–(e) stands for VTP-0, VTP-0.05, VTP-0.5, VTP-1 and VTP-1.2.

Table 1
Binding energy of V, Ti, P and O

Sample	V $2p_{3/2}$/eV	Ti $2p_{3/2}$/eV	P 2p/eV	O 1s/eV	V^{5+}/V^{4+}
VTP-0	517.28	458.93	–	530.28	3.53
VTP-0.05	517.31	459.08	133.97	530.45	3.18
VTP-0.5	517.41	459.30	133.90	531.02	6.58
VTP-1	517.32	459.26	133.87	531.22	4.48
VTP-1.2	517.69	459.31	134.04	531.52	1.33

Table 2
Textural properties of different samples

Sample	Surface area/ $m^2 \cdot g^{-1}$	Average pore size/ nm	Pore volume/ $cm^3 \cdot g^{-1}$
VTP-0	5.45	26.39	0.036
VTP-0.05	7.06	35.13	0.063
VTP-0.5	6.52	27.42	0.035
VTP-1	5.06	21.63	0.029
VTP-1.2	1.52	7.41	0.003
VTP-1 used	4.50	10.86	0.005

tion steps, direct C—C bond breaking is entropically more favorable. Enough external energy input may be required in order to kinetically facilitate the production of anhydride. At an even higher temperatures, the product is further oxidized to small molecules. Thus, temperature is the key factor for the competing of different reaction processes in the oxidation of durene. Rosowski *et al.* [19] believed that the intermediate in the oxidation of methyl aromatics is even more difficult to over-oxidize than the substrate, which could explain the abnormal phenomenon of the conversion rate *versus* temperature.

As the GHSV ratio between durene and air increases, the yield of PMDA increases and then decreases rapidly, while the change of selectivity is small, remaining ~90%. This provides further evidence that at a high temperature the production of anhydride is kinetically favored over the C—C breaking steps.

For the VTP-1 catalyst, this work tested its stability, the result was shown in Fig. 7(b). Clearly, the VTP-1 catalyst maintains its performance after continuous reaction for 300 h.

3.3. In situ FTIR study

In order to obtain even further information of the oxidation of durene, an *in-situ* FTIR analysis was performed. In order to efficiently vaporize the substrate into the instrument and, to compare the reactions with different substrates, the oxidation of *o*-xylene at VTP-1 and VTP-0 was investigated (Fig. 8). For the oxidation of *o*-xylene with VTP-1, when the temperature is 100 °C, 200 °C, and 300 °C, there are strong stretching vibrations of C—H bonds on the benzene ring and C—H of the methyl group between 2880–3070 cm^{-1}. The vibration peaks at 1450 cm^{-1} and 1500 cm^{-1} are ascribed to the stretching vibrations of the C=C bonds of the benzene ring, and the vibration peak at 1469 cm^{-1} reflects the rocking

Table 3
The activity of catalysts with difference in P molar ratio

Sample	Conversion/%	Selectivity/%	Yield/%	TOF × $10^{-3}/s^{-1}$
VTP-0	42.0	80.1	33.64	0.0048
VTP-0.05	40.0	80.6	32.24	0.0047
VTP-0.5	60.3	87.1	52.52	0.0086
VTP-1	82.4	93.2	76.80	0.0142
VTP-1.2	82.1	78.8	64.69	0.0136

Note: Conditions of the reactions: at the temperature of 400 °C, the GHSV of durene and air were 4.6 h^{-1} and 1400 h^{-1} respectively. The result was given as average of three runs.

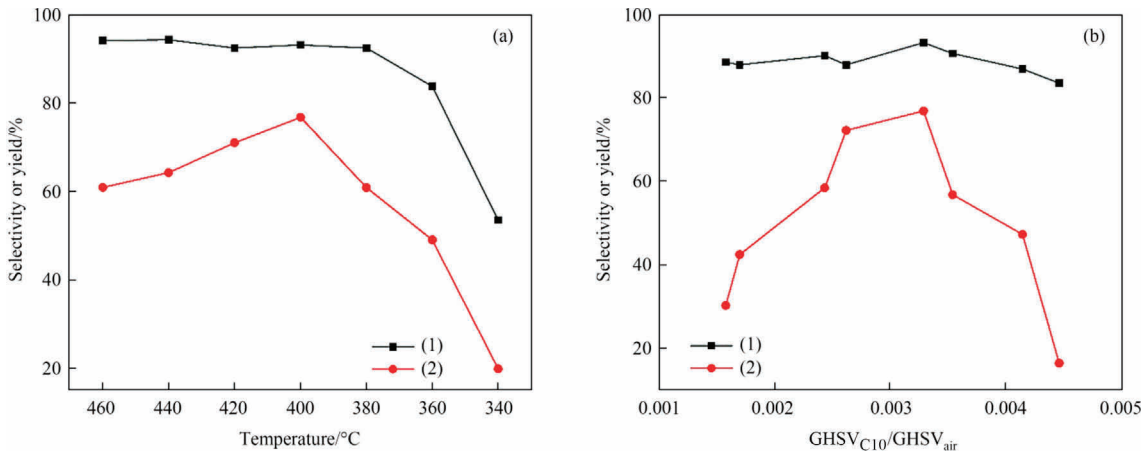

Fig. 6. The effects of temperature and GHSV: (a) for temperature test, the GHSV of durene and air were 4.6 h^{-1} and 1400 h^{-1} respectively; (b) for GHSV effect was tested at the temperature of 400 °C; (1)-selectivity; (2)-yield.

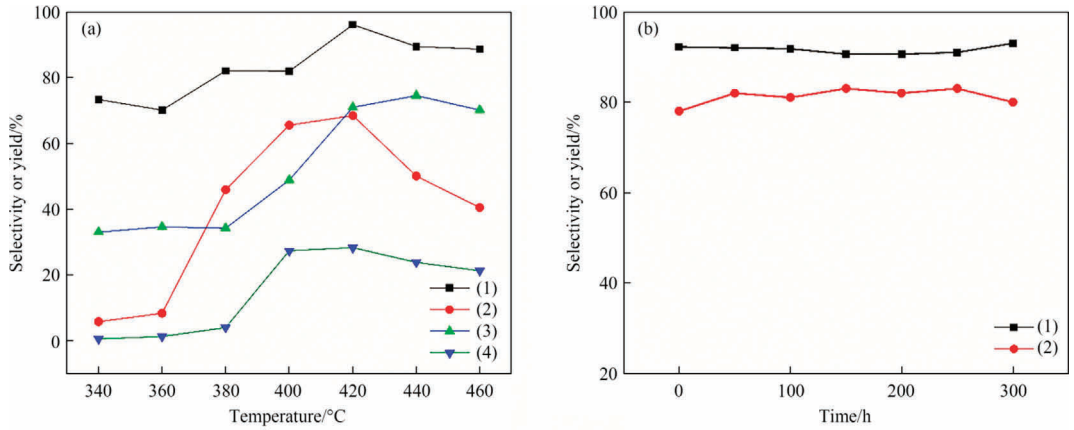

Fig. 7. (a) The oxidation of *o*-xylene and *p*-xylene, the GHSV of *o*-xylene and *p*-xylene is 7.0 h^{-1} and 7.2 h^{-1} (STP), respectively; the GHSV of air is 1000 h^{-1}, (1)- PA selectivity, (2)-PA yield, (3)-PTA selectivity, (4)-yield. (b) The stability of VTP-1 catalyst for oxidation of durene, (1)-selectivity, (2)-yield.

vibration of methyl group. Thus, when the temperature was lower than 300 °C, the methyl group of *o*-xylene was not oxidized completely. At 200 °C and 300 °C, there was an obvious stretching vibration of C—H at 2731 cm^{-1} representing —CHO. This indicated that when reaching 200 °C the oxidation of methyl accelerates dramatically. Further, at 300 °C, the stretching vibration of the C═O bond conjugates with the benzene ring at 1780 cm^{-1}. At 400 °C and 450 °C, there are obvious stretching vibration peaks at 1840 cm^{-1} and 1780 cm^{-1} featured for acid anhydride. In addition, the peak at 1260 cm^{-1} present at 450 °C is the characteristic mark for the vibration of the C—O bond in anhydride. On the other hand, the C═O bond vibration of carboxylic acid (1690 cm^{-1}) is relatively rather weak, indicating that the formation of acid anhydride is not (at least not mainly) contributed by the dehydration of two carboxyl groups. The peak at 1055 cm^{-1} is probably the stretching vibration of the C—O bond in phthalide. Based on the above findings, most likely, after the direct oxidation of $—CH_3$ to —COOH does not take place; rather, the C—H activation concerts with the C—O coupling in an alternative way, which is to be addressed with theoretical calculation.

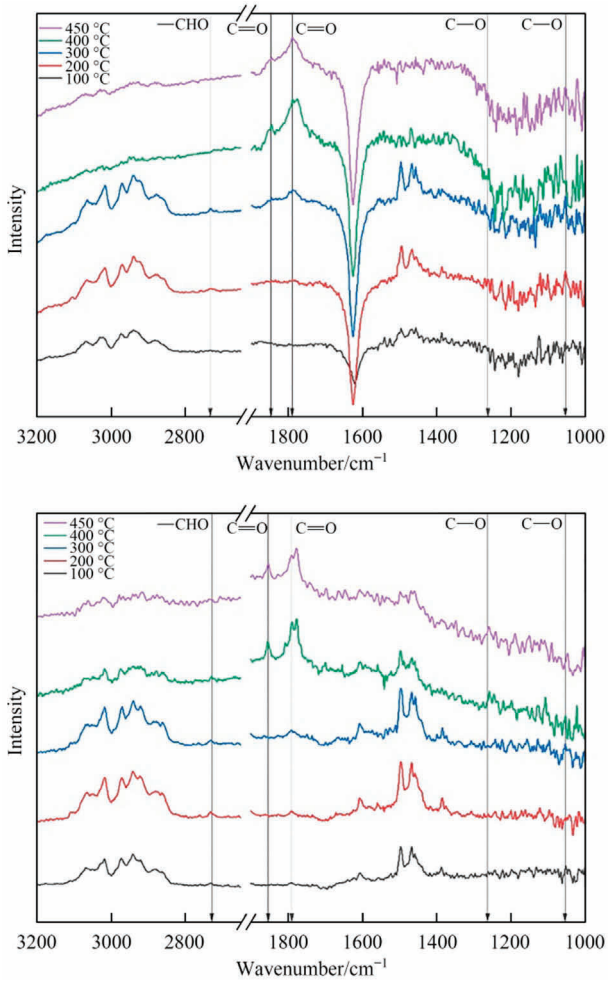

Fig. 8. FTIR difference spectra of VTP-1 (top) and VTP-0 (bottom) catalyst obtained in the oxidation of *o*-xylene.

For the reaction with VTP-0, the fact that *o*-xylene had been oxidized beyond 300 °C is consistent with the result for VTP-1. But two obvious differences exist: first, the conversion of *o*-xylene is lower with VTP-0; second, a typical vibration peak at 1690 cm^{-1} that represents the carboxyl group appears in the spectrum. These evidences suggest that the addition of P element significantly increases the activity of the catalyst and, more interestingly, changes the reaction route.

Further, we also compared the oxidation of *o*-xylene and *p*-xylene under the same conditions (Fig. 7(a)). It turned out that the influence of temperature and GHSV on the oxidation of *o*-xylene and *p*-xylene is similar to that for the oxidation of durene. However, the yield and selectivity of PA are better than the ones for terephthalic acid (PTA), especially in terms of selectivity. This further supports the speculation that the catalytic oxidization of *o*-xylene to PA or durene to PMDA is not a simple dehydration of two carboxyl groups, in line with the *in-situ* FTIR results.

In order to further examine the overall performance of the catalyst prepared in this work, we compared the oxidation of *o*-xylene to phthalic anhydride mediated by VTP-1 with the ones in literatures. As a result, VTP-1 affords relatively high selectivity and yields of phthalic anhydride (for detailed results, see Table S3 in Supplementary Material).

3.4. Theoretical investigation

The reaction mechanisms were interrogated by theoretical calculations. Considering both the preparation process of the VTP-1 catalyst as well as the characterization results, most likely, the vanadium-phosphorus oxides supported on the TiO_2 surface matters for the conversion of durene to pyromellitic dianhydride. Thus, a $V_6P_8O_{36}$ cluster was used for the modeling of the V—P—O species and, for simplification and clarity, the oxidation of *o*-xylene to

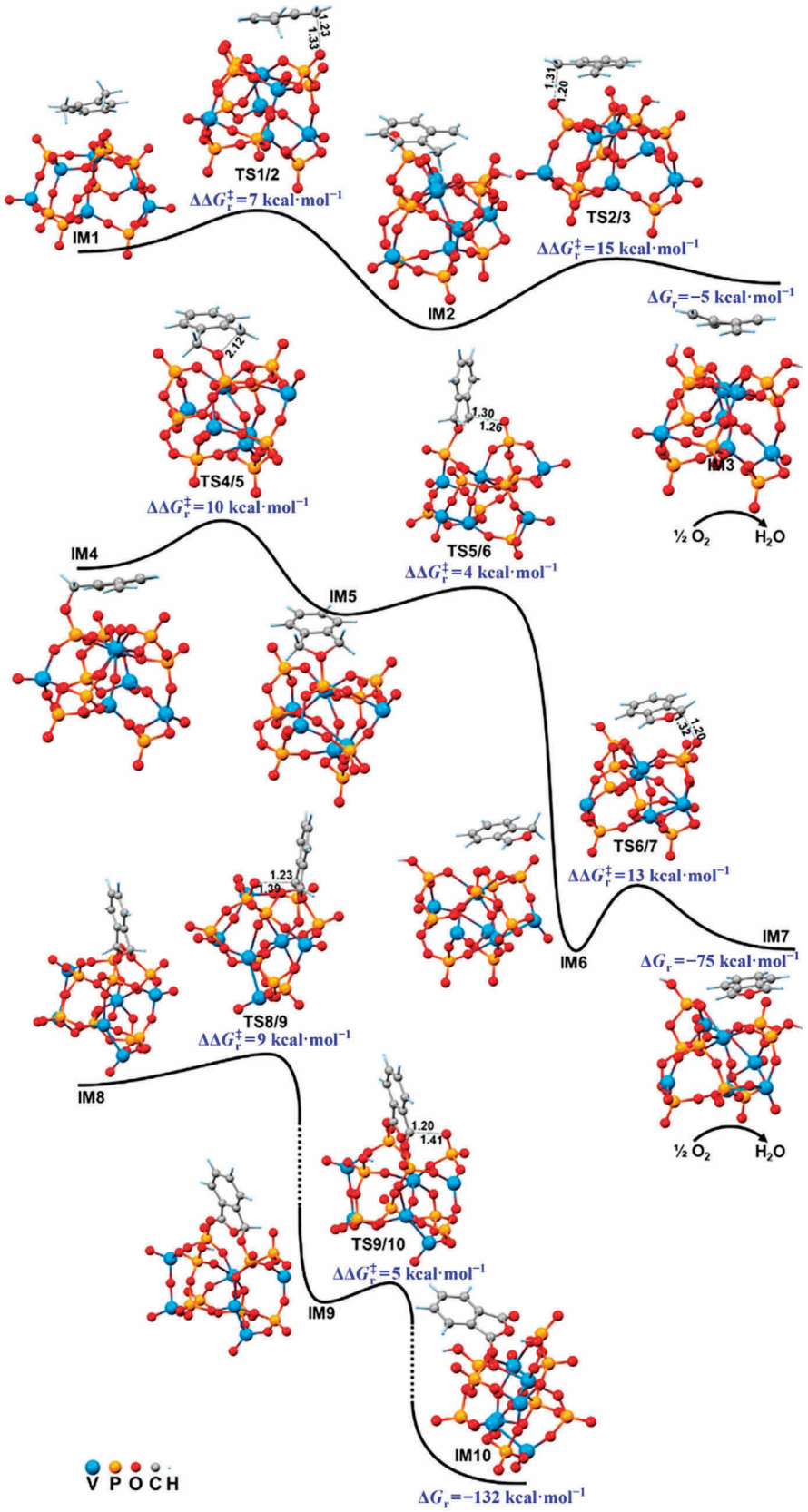

Fig. 9. Simplified PES and selected structural information for the generation of phthalic anhydride mediated by the V—P—O species (1 kcal = 4.186 kJ).

phthalic anhydride was calculated to understand in detail the C—H activation and C—O coupling processes.

As shown in Fig. 9, initially C—H bond activation of the two methyl groups takes place upon hydrogen transfer from the carbon atoms to two P—O sites, respectively (IM1→IM3). Spontaneous C—O coupling is possible when the reaction site is oxidized by external oxygen, generating IM4. Next, a five-member ring forms by making a second C—O bond at the same oxygen atom (IM4 → IM5) to form a benzofuran molecule. This step is followed by further, step-wise dehydrogenation of the methylene groups, thus generating IM7. Again, formation of another two C—O bonds occurs when removing the hydrogen atoms from the newly formed hydroxyl groups (IM8). Finally, by eliminating a third pair of hydrogen atoms from the substrate, an intact pyromellitic dianhydride molecule is produced (IM10). For the entire process from IM1 to IM10, it is thermodynamically favorable due to its high exothermicity. In addition to the pathways shown in Fig. 9, alternative ones were also found; however, they are energetically less favorable (See Fig. S6 in the Supplementary Material).

Further, we compared theoretically the catalytic activity of the V—P—O species with that of V_2O_5. As shown in Fig. 10, upon interaction of the durene molecule with the V_2O_5 cluster (a $V_{14}O_{35}$ model), breaking of the C—H bonds of the two methyl groups proceeds continuously until the phthalic acid molecule forms, that is,

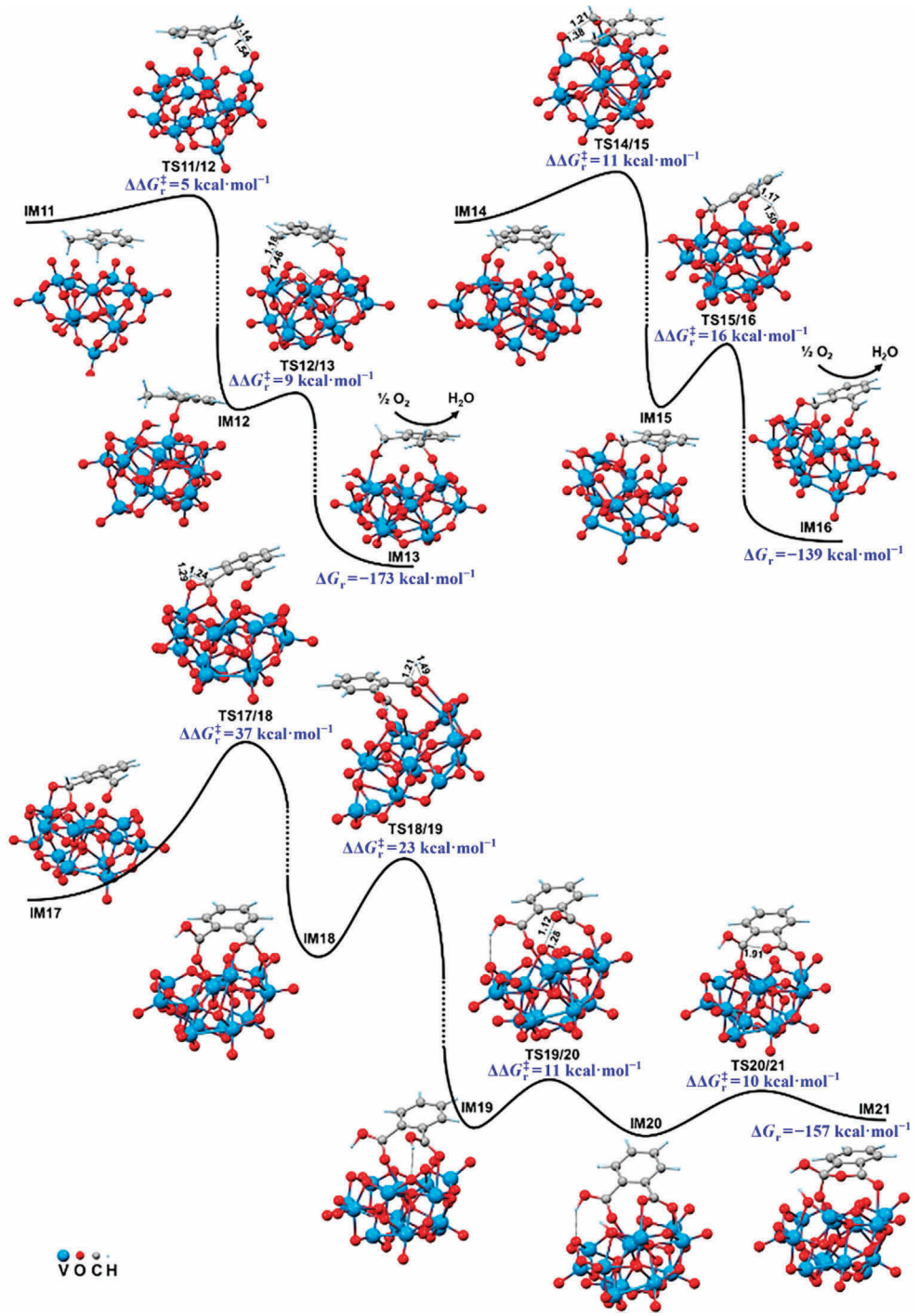

Fig. 10. Simplified PES and selected structural information for the generation of phthalic anhydride mediated by V_2O_5 cluster.

IM11→IM19. Subsequent hydrogen migration between the oxygen atoms concerts with the ring-closing step, thus forming the phthalic anhydride equivalent species (IM21). Here, though we tried to find a pathway in which a five-member ring forms precedingly before the carbonyl groups are generated, a benzofuran intermediate analogous to IM5 in the V-P-O/*o*-xylene system cannot be found. Rather, after IM16 is generated, the C—O coupling to form a five-member ring is possible (See Fig. S7 in the Supplementary Material). However, the associated reaction pathways is energetically less competing with the ones shown in Fig. 10.

As compared with the reaction in the V—P—O/*o*-xylene system, the initial C—H activation of the methyl group in the V_2O_5/*o*-xylene system is even more favorable both kinetically and thermodynamically. However, further C—H activation to form the carbonyl equivalent species in the V_2O_5/*o*-xylene system is kinetically less favorable. This is in line with the experimental finding in the oxidation of durene that the VTP-1 catalyst outperformed VTP-0. Considering the difference of the reaction pathways presented in Fig. 9 and Fig. 10, most likely, the key role phosphorus plays in the formation of anhydride can be attributed to the *in-situ* formation of the benzofuran intermediate. We also tried to calculate the interaction of *o*-xylene with a P-rich site, and it turned out that the phenyl ring is prone to be activated as the C—O coupling therein is facilitated. Thus, while doping P in the V_2O_5 cluster indeed increases the catalytic activity, an over-high P:V ratio may also facilitate the side reactions thus decreasing the selectivity of anhydride, in line with the experimental findings. Finally, though we cannot list and calculate all possible C—C activation routes for *o*-xylene, we selected one conceivable one and compared the associated thermochemistry in the V—P—O/*o*-xylene and V_2O_5/*o*-xylene systems (see Figs. S8 and S9 in Supplementary Material). Consequently, the C—C activation process in V—P—O/*o*-xylene is less favored as compared to the generation of phthalic anhydride both kinetically and thermodynamically. For the V_2O_5/*o*-xylene system, however, the C—C cleavage of the phenyl ring is kinetically more competing. These results are in line with the experimental performances of the VTP-1 and VTP-2 catalysts in the oxidation of durene.

4. Conclusions

In summary, a V-Ti-P ternary catalyst for the oxidation of durene and *o*-xylene to the associated anhydrides was prepared by doping P with V upon deposition on TiO_2. A P:V = 1:1 ratio turned out to afford good selectivity and yield for the synthesis of PMDA *via* continuous oxidation of durene in the gaseous phase: the selectivity of PMDA in the liquid products is up to 93%, corresponding to a yield of 77%. The catalyst was characterized by XRD, XPS, and Raman, and all evidences indicated that the addition of P converts part of the active vanadium species to $VOPO_4$ upon slight increase of the valence state of V. *Via in-situ* FTIR, the mechanistic aspects was explored using *o*-xylene as the substrate. The analysis indicated that the dehydration of phthalic acid may not count much for the production of anhydride, while theoretical calculation revealed that the intermediate benzofuran is generated at a P site in the production of anhydride. By contrast, however, without P the dehydration of phthalic acid is more favorable. Moreover, the addition of P decreases the reaction barriers of the C—H activation steps, while otherwise the C—C breaking pathway is even more competing. Considering the short residence time and the high yield, efficient production of PMDA is facilitated.

Data Availability

Data will be made available on request.

Declaration of Competing Interest

The authors declare that they have no known competing financial interests or personal relationships that could have appeared to influence the work reported in this paper.

Acknowledgements

Generous financial support by the National Natural Science Foundation of China (21878265).

Supplementary Material

Supplementary data to this article can be found online at https://doi.org/10.1016/j.cjche.2022.03.026.

References

[1] M.A.R. Matos, M.S. Miranda, S.M.M. Pereira, V.M.F. Morais, J.F. Liebman, The experimental and calculational thermochemistry of 1,2,4,5-benzenetetracarboxylic dianhydride: Is this 10 pi multiring species aromatic?, *J Phys. Chem. A* 111 (30) (2007) 7181–7188.
[2] R.T. Guo, Y. Wang, S. Heng, G.B. Zhu, V.S. Battaglia, H.H. Zheng, Pyromellitic dianhydride: A new organic anode of high electrochemical performances for lithium ion batteries, *J. Power Sources* 436 (2019) 226848.
[3] V.V. Kaichev, G.Y. Popova, Y.A. Chesalov, A.A. Saraev, D.Y. Zemlyanov, S.A. Beloshapkin, A. Knop-Gericke, R. Schlögl, T.V. Andrushkevich, V.I. Bukhtiyarov, Selective oxidation of methanol to form dimethoxymethane and methyl formate over a monolayer V_2O_5/TiO_2 catalyst, *J. Catal.* 311 (2014) 59–70.
[4] V.V. Kaichev, Y.A. Chesalov, A.A. Saraev, A.Y. Klyushin, A. Knop-Gericke, T.V. Andrushkevich, V.I. Bukhtiyarov, Redox mechanism for selective oxidation of ethanol over monolayer V_2O_5/TiO_2 catalysts, *J. Catal.* 338 (2016) 82–93.
[5] T. Zhang, R.R. Zhang, Y.K. Zhang, Z.Q. Xie, Y.W. Li, H. Wu, F. Dai, R.X. Liu, Phosphoric acid: A key role in control of structure and properties of vanadium phosphorus oxide catalysts during synthesis, *ChemistrySelect* 6 (4) (2021) 513–521.
[6] R. Marx, H.J. Wölk, G. Mestl, T. Turek, Reaction scheme of *o*-xylene oxidation on vanadia catalyst, *Appl. Catal. A Gen.* 398 (1–2) (2011) 37–43.
[7] T. Aycan, F. Öztürk, H. Paşaoğlu, Investigation of structural, spectral and thermal properties of one-dimensional polymer containing pyromellitic acid and isonicotinamide, *J. Mol. Struct.* 1176 (2019) 685–694.
[8] W.P. Schammel, D.K. John, Process for the production of trimellitic acid and pyromellitic acid by staged bromine addition in an oxidation of polyalkylaromatics, USA Pat., 4755622 (1985).
[9] B.I. Kutepov, B.S. Bal'zhinimaev, Reasons for the deactivation of vanadia-titania catalysts for partial durene oxidation during prolonged performance, *Kinet. Catal.* 42 (3) (2001) 291–300.
[10] B.A. Moiseevich, K.V. Viktorovich, S.R. Gazimovich, N.V. Filippovich, N.E. Nikolaevna, A.J. Mikhajlovich, Method of producing intramolecular anhydrides of benzene polycarboxylic acids, Rusian Pat., 2412178 (2009).
[11] Y. Hu, N. Li, G. Li, A. Wang, Y. Cong, X. Wang, T. Zhang, Sustainable production of pyromellitic acid with pinacol and diethyl maleate, *Green Chem.* 19 (7) (2017) 1663–1667.
[12] F. Cavani, C. Cortelli, A. Frattini, B. Panzacchi, V. Ravaglia, F. Trifiro, C. Fumagalli, R. Leanza, G. Mazzoni, The characterization of the V species and the identification of the promoting effect of dopants in V/Ti/O catalysts for *o*-xylene oxidation, *Catal. Today* 118 (3–4) (2006) 298–306.
[13] A. Akbari, S.M. Alavi, The effect of cesium and antimony promoters on the performance of Ti-phosphate-supported vanadium(V) oxide catalysts in selective oxidation of *o*-xylene to phthalic anhydride, *Chem. Eng. Res. Des.* 102 (2015) 286–296.
[14] G.J. Hutchings, Heterogeneous catalysts-discovery and design, *J. Mater. Chem.* 19 (9) (2009) 1222–1235.
[15] N. Ballarini, A. Brentari, F. Cavani, S. Luciani, C. Cortelli, F. Cruzzolin, R. Leanza, A revision of the mechanism of *o*-xylene oxidation to phthalic anhydride with V/Ti/O catalysts, and the role of the promoter Cs, *Catal. Today* 142 (3–4) (2009) 181–184.
[16] G. Deo, I.E. Wachs, Effect of additives on the structure and reactivity of the surface vanadium oxide phase in V_2O_5/TiO_2 catalysts, *J. Catal.* 146 (2) (1994) 335–345.
[17] B. Grzybowska-Swierkosz, Effect of additives on the physicochemical and catalytic properties of oxide catalysts in selective oxidation reactions, *Top. Catal.* 21 (1–3) (2002) 35–46.
[18] J. Jimenez-Jimenez, J. Merida-Robles, E. Rodriguez-Castellon, A. Jimenez-Lopez, M.L. Granados, S. del Val, I.M. Cabrera, J.L.G. Fierro, Oxidation of *o*-xylene on mesoporous Ti-phosphate-supported VO_x catalysts and promoter effect of K^+ on selectivity, *Catal. Today* 99 (1–2) (2005) 179–186.
[19] F. Rosowski, S. Altwasser, C.K. Dobner, S. Storck, J. Zühlke, H. Hibst, New silver- and vanadium-containing multimetal oxides for oxidation of aromatic hydrocarbons, *Catal. Today* 157 (1–4) (2010) 339–344.

[20] C.B. Rodella, V.R. Mastelaro, Structural characterization of the V_2O_5/TiO_2 system obtained by the sol-gel method, *J. Phys. Chem. Solids* 64 (5) (2003) 833–839.
[21] A. Gervasini, P. Carniti, J. Keranen, L. Niinisto, A. Auroux, Surface characteristics and activity in selective oxidation of *o*-xylene of supported V_2O_5 catalysts prepared by standard impregnation and atomic layer deposition, *Catal. Today* 96 (4) (2004) 187–194.
[22] S.K. Maurya, P. Patil, S.B. Umbarkar, M.K. Gurjar, M. Dongare, S. Rudiger, E. Kemnitz, Vapor phase oxidation of 4-fluorotoluene over vanadia-titania catalyst, *J. Mol. Catal. A Chem.* 234 (1–2) (2005) 51–57.
[23] O. Richter, G. Mestl, Deactivation of Commercial, High-load *o*-xylene feed VO_x/TiO_2 phthalic anhydride catalyst by unusual over-reduction, *Catalysts* 9 (5) (2019) 435.
[24] L. Abello, E. Husson, Y. Repelin, G. Lucazeau, Vibrational spectra and valence force field of crystalline V_2O_5, *Spectrochim. Acta A Mol. Spectrosc.* 39 (7) (1983) 641–651.
[25] F. Benabdelouahab, R. Olier, N. Guilhaume, F. Lefebvre, J.C. Volta, A study by *in situ* laser Raman-spectroscopy of VPO catalysts for normal-butane oxidation to maleic-anhydride. 1. Preparation and characterization of pure reference phases, *J. Catal.* 134 (1) (1992) 151–167.
[26] M. Sambi, G. Sangiovanni, G. Granozzi, F. Parmigiani, Growth and the structure of epitaxial VO_2 at the TiO_2(110) surface, *Phys. Rev. B* 55 (12) (1997) 7850–7858.
[27] V. Lochař, H. Drobná, FTIR study of the interaction of crotonaldehyde and maleic anhydride with V_2O_5 and MoO_3, *Appl. Catal. A Gen.* 269 (1–2) (2004) 27–31.